Escherichia coli K12 Strain JW5917-1, an *rcsC* Knock Out Strain in the Keio Collection, Displays an Impaired Growth Phenotype Compared to its Isogenic Parent Strain BW25113

Kyler Kanegawa, Emma McIver, Jackson Moore, Matthew A. Tester

Department of Microbiology and Immunology, University of British Columbia, Vancouver, British Columbia, Canada

SUMMARY The Regulator of Capsule Synthesis (Rcs) phosphorelay pathway regulates the expression of genes necessary for biofilm formation and stress response within Enterobacteriaceae. RcsC, an inner membrane sensor kinase, autophosphorylates during periods of antibiotic stress, osmotic stress, and nutrient deprivation. This leads to activation of downstream components, such as *rprA* and RpoS, which are important for regulating the stress response. Previous work has suggested a linkage between the Rcs pathway and resistance to antibiotics targeting the cell wall. In this study, we characterized the Keio collection knockout mutants JW5917-1, JW0192-1, JW2204-1, JW2205-2 which encode deletions of *rcsC, rcsF, rcsD* and *rcsB*, respectively. Using PCR and Sanger sequencing we mapped the site-specific insertion of the kanamycin-resistance cassette defining the Δ*rcsC* mutant. We observed reduced growth yields associated with the Δ*rcsC* mutant, which appear to be a distinct phenotype relative to the wildtype parent strain BW25113. We also observed that the Δ*rcsF* mutant shows increased sensitivity to penicillin compared to the other Δ*rcs* strains.

INTRODUCTION

The Regulator of Capsule Synthesis (Rcs) phosphorelay pathway is a conserved multicomponent signal transduction system in Enterobacteriaceae. Five major proteins are involved in the Rcs pathway: the outer membrane lipoprotein RcsF, inner membrane sensor kinase RcsC, inner membrane phosphotransferase RcsD, and the intracellular response regulators RcsB/RcsA (Figure 1). Rcs pathway activation is triggered by stress to the peptidoglycan layer of the bacterial cell wall, conferring intrinsic antibiotic resistance to β-lactam antibiotics (1). Phosphorylated RcsA/RcsB complexes regulate the expression of the *cps* operon involved in synthesis of capsular polysaccharides, and phosphorylated RcsB regulates expression of multiple genes involved in the bacterial stress response including *rprA*, a small noncoding RNA that promotes RpoS translation (2, 3). Otherwise known as σ38, RpoS is a sigma factor that regulates over 500 genes in response to various stress stimuli including nutritional deprivation, osmotic stress, and antibiotics (4, 5).

It is thought that signal transduction begins at RcsF, leading to the autophosphorylation of RcsC by removal of RcsC-inhibiting protein IgaA (6). Membrane bound RcsC transfers a phosphate to RcsD, an intermediary phosphotransferase, via a kinase domain. RcsD subsequently phosphorylates response regulators RcsB and RcsA (6). Previous research has identified RcsF-independent pathways within *Escherichia coli* that activate capsule synthesis (7, 8). DjlA, a membrane-protein within the DnaJ chaperone family has been demonstrated to induce expression of the *cps* operon through RcsC but not RcsF (7). Additionally, the lipoprotein YpdL has been shown to activate the Rcs pathway independent of RcsF, leading to the production of capsular polysaccharides (8). The true nature of the Rcs pathway is complex and likely interwoven with multiple signalling pathways (6).

Without induction of the Rcs pathway, *E. coli* exhibits planktonic growth with prominent motility (6). Upon Rcs pathway activation, capsule and biofilm synthesis increases and the cell shifts to stable, non-motile growth while fixed to an environmental surface (6). Biofilm formation enhances bacterial growth in the presence of antibiotic and contributes to cell survival during nutrient deprivation (9). Previous research on knockout *rcsC*, *rcsD*, and *rcsF E. coli* mutants has demonstrated impaired activation of the Rcs

Published Online: 17 September 2019

Citation: Kanegawa K, McIver E, Moore J, Tester MA. 2019. *Escherichia coli* K12 Strain JW5917-1, an *rcsC* Knock Out Strain in the Keio Collection, Displays an Impaired Growth Phenotype Compared to its Isogenic Parent Strain BW25113. UJEMI 24:1-9

Editor: Julia Huggins, University of British Columbia

Address correspondence to: https://jemi.microbiology.ubc.ca/

system following induction with antibiotics as they lack the ability to activate expression of the *cps* operon and induce biofilm formation (10). To the best of our knowledge, investigation into the growth phenotype of a knockout *rcsC E. coli* mutant in the presence or absence of penicillin had yet to be conducted.

The Keio Collection is a complete collection of *E. coli* K12 strain BW25113 single gene knockout mutants for all non-essential genes (11). Knockout mutants were constructed by replacement of a target gene with a kanamycin-resistance cassette (*kanR*), contained within the pKD13 plasmid. Primers were designed with 5' overhangs homologous to downstream and upstream portions of the target gene and resulted in the amplification of *kanR* from pKD13. *kanR* was then inserted into the genome at the designated genes by homologous recombination with excision of the target gene.

The aim of this study was to elucidate the construction of the Δ*rcsC* mutant obtained from the Keio Collection, and to determine the strain's growth characteristics in the presence and absence of penicillin. Additionally, this study represents an initial step towards defining an experimental system to characterize the role of RcsF in cellular responses to environmental stress.

METHODS AND MATERIALS

Bacterial strains. All strains described in this investigation were ordered from the Keio Collection of the Yale Coli Genetic Stock Center (Table 1). *Escherichia coli* K12 strain BW25113 was designated as the wildtype (WT) strain in this study, as knockout mutants were constructed using BW25113 as the parent strain (11). Δ*rcsF*, Δ*rcsC*, Δ*rcsD*, and Δ*rcsB* knockout mutants were utilized in characterization of the Δ*rcsC* mutant. WT was plated on LB agar plates, and each knockout mutant was plated on LB agar supplemented with 50 µg/mL kanamycin. Liquid cultures of all strains were grown in LB at 37 °C with agitation.

Antibiotic stock solutions. Concentrated stock solutions of kanamycin sulfate and penicillin were prepared by dissolving powdered antibiotic in distilled water and sterilizing with a 0.22 µm nitrocellulose filter. Antibiotic stocks were stored at –20 °C.

Genomic DNA extraction. Overnight cultures of WT and the Δ*rcsC* mutant were centrifuged at 4000 x g for 5 minutes, and genomic DNA was extracted using the PureLink Genomic DNA Mini Kit (Invitrogen K1820-01). Genomic DNA was stored at –20 °C.

Primer design. To characterize the deletion of *rcsC* in the Δ*rcsC* mutant, primers were designed for PCR (Table 2). Two primers complementary to upstream and downstream

TABLE 1 Summary of *E. coli* K12 strains and corresponding genotypes used in this study.

Strain	Designation	Genotype
BW25113	Wildtype (WT)	*Δ(araD-araB)567, ΔlacZ4787*(::rrnB-3), *λ⁻*, *rph-1*, *Δ(rhaD-rhaB)568*, *hsdR514*
JW0192-1	Δ*rcsF*	F-, *Δ(araD-araB)567*, *ΔrcsF721::kan*, *ΔlacZ4787*(::rrnB-3), *λ⁻*, *rph-1*, *Δ(rhaD-rhaB)568*, *hsdR514*
JW5917-1	Δ*rcsC*	F-, *Δ(araD-araB)567*, *ΔlacZ4787*(::rrnB-3), *λ⁻*, *ΔrcsC771::kan*, *rph-1*, *Δ(rhaD-rhaB)568*, *hsdR514*
JW2204-1	Δ*rcsD*	F-, *Δ(araD-araB)567*, *ΔlacZ4787*(::rrnB-3), *λ⁻*, *ΔrcsD769::kan*, *rph-1*, *Δ(rhaD-rhaB)568*, *hsdR514*
JW2205-2	Δ*rcsB*	F-, *Δ(araD-araB)567*, *ΔlacZ4787*(::rrnB-3), *λ⁻*, *ΔrcsB770::kan*, *rph-1*, *Δ(rhaD-rhaB)568*, *hsdR514*

TABLE 2 Sequence, Melting Temperature, and % GC Content of Primers.

Primer	Sequence (5'-3')	Tm (°C)	% GC Content
rcsC-F	gtaaacgccttatccggcctacg	61	57
rcsC-R	tttctcggcggtgtatcatattcca	59	44
kanR-R	gctcgatgcgatgtttcgctt	60	51

portions of the BW25113 *rcsC* gene (rcsC-F and rcsC-R, respectively) were designed to amplify a PCR product of size 2.9 kbp in the WT strain. The kanR-R primer was designed to be complementary to the 5' portion of *kanR*. kanR-R and rcsC-R were used together to amplify a PCR product of size 3.2 kbp in the Δ*rcsC* mutant.

PCR and gel electrophoresis. PCR was performed using the Invitrogen Platinum Taq DNA Polymerase (Invitrogen 10966-018). Each PCR reaction consisted of 5 µL 10x Reaction Buffer, 1.5 mM $MgCl_2$, 1 mM dNTPs, 0.4 µM primers, 0.2 µL Platinum Taq Polymerase, and 10 ng template DNA. PCR amplification was executed using the following thermocycler parameters: initial denaturation for 2 minutes at 95 °C; 30 cycles of denaturation for 30 seconds at 95 °C, primer annealing for 1 minute at 55 °C, extension for 3.25 minutes at 72 °C, and a final extension for 5 minutes at 72 °C. PCR was conducted on a Bio-Rad T100 Thermocycler. To validate PCR conditions, pUC19 (Invitrogen 15364-01) was utilized as a positive control. To validate primer design, a no-template negative control with each primer pair was conducted. Gel electrophoresis was performed on a 1.5% w/v

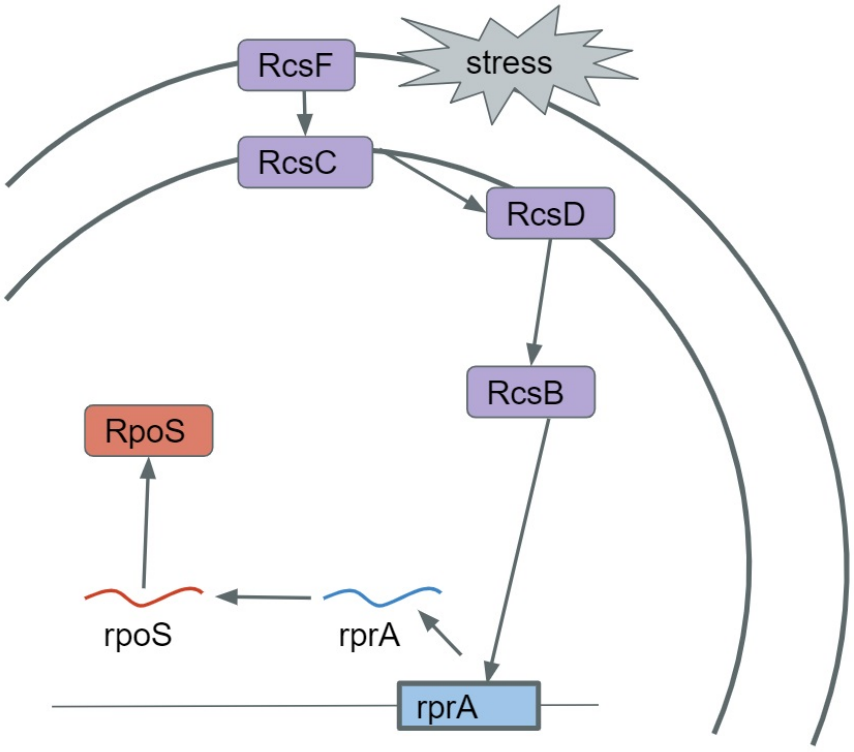

FIG. 1 Proposed Rcs signalling pathway in response to antibiotic stress, adapted from Jalalkamali *et al*. The RcsD membrane bound protein is a phosphotransferase that activates the DNA binding activity of RcsB. RcsB is a transcription factor that increases the expression of the microRNA *rprA*. *rprA* mRNA stabilizes *rpoS* mRNA to increase the translation of RpoS, a sigma factor. It is still not known exactly how RcsC and RcsF fit into this signalling pathway in response to extracellular and intracellular types of antibiotic stress.

agarose gel with 1x TAE buffer at 110 V for 1 hour. PCR products were stained using SYBR Green (Invitrogen S7563) and visualized with a BioRad ChemiDoc MP Imaging System.

PCR clean-up and sequencing. PCR products were purified using the GeneJET PCR Purification kit (Thermo Scientific K0702). Samples were submitted to GENEWIZ for Sanger sequencing using 60 ng of DNA template and 5 µM of the kanR-R primer. Sequence analysis and annotation was conducted using SnapGene Viewer.

Growth curve. To determine the relative growth yield of each strain, growth analysis was performed on WT, Δ*rcsF*, Δ*rcsC*, Δ*rcsD*, and Δ*rcsB* cultures in the presence and absence of penicillin. Overnight cultures of each strain were diluted 100x in LB and 200 µL of each diluted culture was placed into respective wells in a 96-well plate. Each strain was treated with the following treatments of penicillin: 0 µg/mL, 10 µg/mL, 30 µg/mL and 60 µg/mL. Each treatment was conducted in triplicate. Growth curves were generated by incubating the cells at 37 °C and measuring the OD_{600} of the cultures every 10 minutes for 24 hours using a BioTek Synergy Microplate Reader.

RESULTS

The *rcsC* gene was partially deleted in the Δ*rcsC* mutant, with *kanR* insertion at the 5' end of *rcsC*. To investigate the size of the deleted *rcsC* gene region in the Δ*rcsC* mutant, the *rcsC* gene was amplified from genomic DNA of the Δ*rcsC* strain using PCR. As previously described, two primer sets were used: primers flanking either side of the *rcsC* gene (rcsC-F/rcsC-R), and a primer for the 5' end of *kanR* (kanR-R) and the rcsC-R primer. The rcsC-F/rcsC-R primer set was also used to amplify the *rcsC* gene in WT for comparison. The resulting agarose gel showed three bright bands of similar size (Figure 2). The largest product was the rcsC-F/rcsC-R amplicon from the Δ*rcsC* mutant, then the rcsC-R/kanR-R amplicon from the Δ*rcsC* mutant, with the rcsC-F/rcsC-R amplicon from the WT

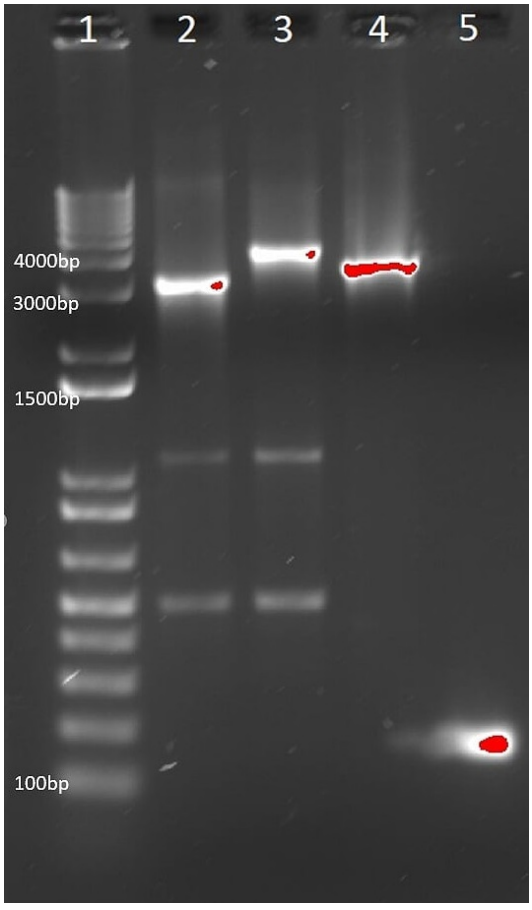

FIG. 2 Results of PCR of *rcsC* locus using different primer sets on either wildtype or Δ*rcsC* strains. Lane 1: 1kb+ DNA ladder (Thermofisher); lane 2: rcsC-F and rcsC-R primers against WT genome; Lane 3: rcsC-F and rcsC-R primers against Δ*rcsC* genome; lane 4: kanR-R and rcsC-R primers against Δ*rcsC* genome; lane 5: positive control (pUC19).

being the smallest. A set of two smaller bands can be seen in the rcsC-F/rcsC-R amplicons from the WT and Δ*rcsC* mutant in lanes 2 and 3 of Figure 2. Using gradient PCR these amplicons disappeared at an annealing temperature of 56 °C and above (data not shown) and are likely non-specific by-products.

The PCR product from the Δ*rcsC* strain created using the rcsC-R/kanR-R primer set was purified, and Sanger sequencing was performed. Using BLAST, we compared the resulting sequence to the *rcsC* gene and found 18% of our sequence aligned, while the remaining 82% aligned with *kanR* (Figure 3). The sequence of the reverse primer used by Baba *et al* (2006) to generate the Δ*rcsC* mutant is present immediately after the junction between the *kanR* sequence and the *rcsC* sequence; however, the sequence of the forward primer used by Baba *et al* is not present within our sequence. This fits our expectations as our kanR-R primer bound downstream of the beginning of the *kanR*, which is where we would expect to find this forward primer sequence contained within the *rcsC* sequence. We found that a 354 bp segment of *rcsC*, which contained the gene's +1 site, was excised and replaced with *kanR*. In the process, the *kanR* was fused with the remaining downstream 2476 bp of *rcsC*. However, this downstream portion of *rcsC* cannot be transcribed because the *kanR* insert contains a transcription termination sequence. Therefore, unlike most of the mutants generated within the Keio Collection, the *rcsC* gene was not excised completely and replaced. Instead, *kanR* replaced the *rcsC* transcription start sequence, disallowing *rcsC* transcription and resulting in no RcsC protein product (Figure 3).

Relative growth of Δ*rcs* mutants in LB media demonstrated decreased growth yield of the Δ*rcsC* mutant in no antibiotic stress. To further characterize the Rcs pathway, we set to investigate the growth characteristics of our mutants, Δ*rcsC,* Δ*rcsB*, Δ*rcsD*, and Δ*rcsF*, compared to WT. When we compared the relative growth rates and yields with no antibiotic, there was no qualitative difference between Δ*rcsB*, Δ*rcsD*, and Δ*rcsF* strains compared to WT; however, the Δ*rcsC* mutant showed a slower exponential growth and final yield, as measured by optical density (OD_{600}) at stationary phase, compared to the WT strain and the other mutants (Figure 4). Therefore, in conditions of no antibiotic stress the Δ*rcsC* mutant is negatively impacted in growth while other Δ*rcs* mutants are not.

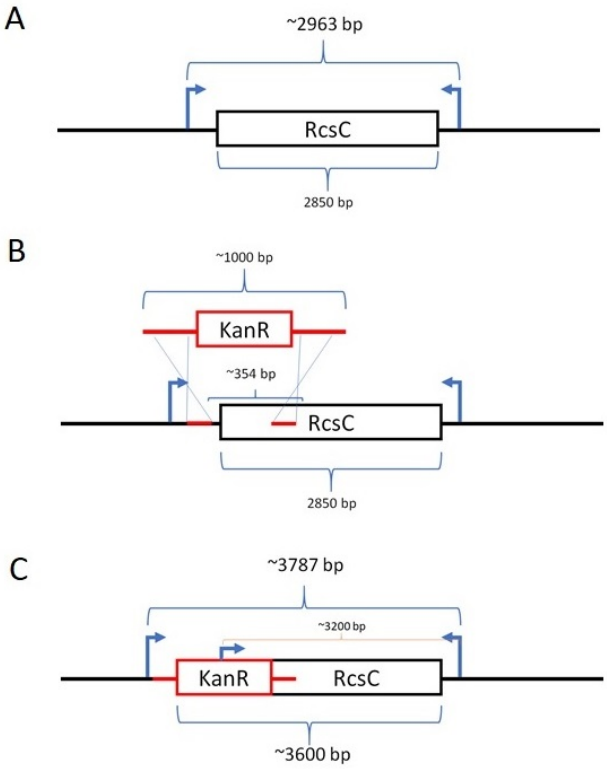

FIG. 3 Diagram of kanamycin gene insertion mechanism for the generation of the Δ*rcsC* mutant JW5917-1 as adapted from Baba *et al*. **A)** WT *rcsC* gene (black) and *rcsC* flanking primer set (blue). The *rcsC* ORF is 2850 bp and the PCR product is ~2963bp. **B)** Site of *kanR* insertion into WT *rcsC* gene to make Keio Collection strain Δ*rcsC* knockout. Red is the kanamycin resistance gene and sites of homologous recombination. The size of the spliced-out portion of *rcsC* is ~354bp and the *kanR insert* is ~1000bp. **C)** The final Keio Collection Δ*rcsC* product after homologous recombination. After insertion, the total PCR product using RcsC-F/RcsC-R primers are 3787bp. The product using the RcsC/KanR primer set is ~3200 bp.

With increasing penicillin concentrations all Δ*rcs* mutants and WT show inhibited growth, but at varying degrees. Penicillin was used to assess the ability of the Δ*rcs* mutants to grow during periods of antibiotic stress. As well, penicillin is known to be a potent activator of the Rcs pathway (3). When comparing the growth of the Δ*rcsC* mutant exposed to different concentrations of penicillin, there was little observable difference in growth rate and yield between 0 µg/mL and 10 µg/mL of penicillin (Figure 5). However, when the penicillin concentration was increased to 30 µg/mL and 60 µg/mL we saw a marked decrease in yield (Figure 5), as well as an increase in the time to initiate exponential growth phase from lag phase (data not shown). Similar observations were found in the other knockout strains, but a penicillin concentration of 30 µg/mL did not affect the yield of the Δ*rcsB* and Δ*rcsD* mutants (Figure 5). At a penicillin concentration of 60 µg/mL we saw a reduction in yield (Figure 5) and an increase in the time to initiate exponential growth phase from lag phase in all strains (data not shown), although the Δ*rcsF* and Δ*rcs*C mutants had notably lower OD_{600} values at all time points.

Increased sensitivity of Δ*rcsF* mutant to penicillin compared to other strains. Increasing the concentration of penicillin from 10 µg/mL to 30 µg/mL increased the exponential growth phase initiation time from lag phase for all mutants by approximately 500 minutes (data not shown). Similarly, the increase in concentration of penicillin from 30 µg/mL to 60 µg/mL increased the transition point from lag to exponential growth phase from 500 minutes to 1000 minutes in all strains (data not shown). The Δ*rcsF* mutant appeared to be more sensitive to increasing concentrations of penicillin relative to the other mutants and WT strain. With no exposure to penicillin, Δ*rcsF* followed a similar growth pattern as the Δ*rcsB* and Δ*rcsD* mutants and WT strains, with the Δ*rcsC* mutant having a markedly lower growth yield at stationary phase (Figure 5). However, when exposed to a penicillin concentration of 30 µg/mL, the Δ*rcsF* mutant demonstrated a decreased concentration of cells in stationary phase, with a comparable OD_{600} value at 1400 minutes to the Δ*rcsC* mutant (Figure 5). Compared to WT and the other Δ*rcs* strains, the Δ*rcsF* mutant demonstrated the greatest change in yield with increasing penicillin concentrations with a 2-fold decrease in OD_{600} at stationary phase between 0 µg/mL and 60 µg/mL of penicillin.

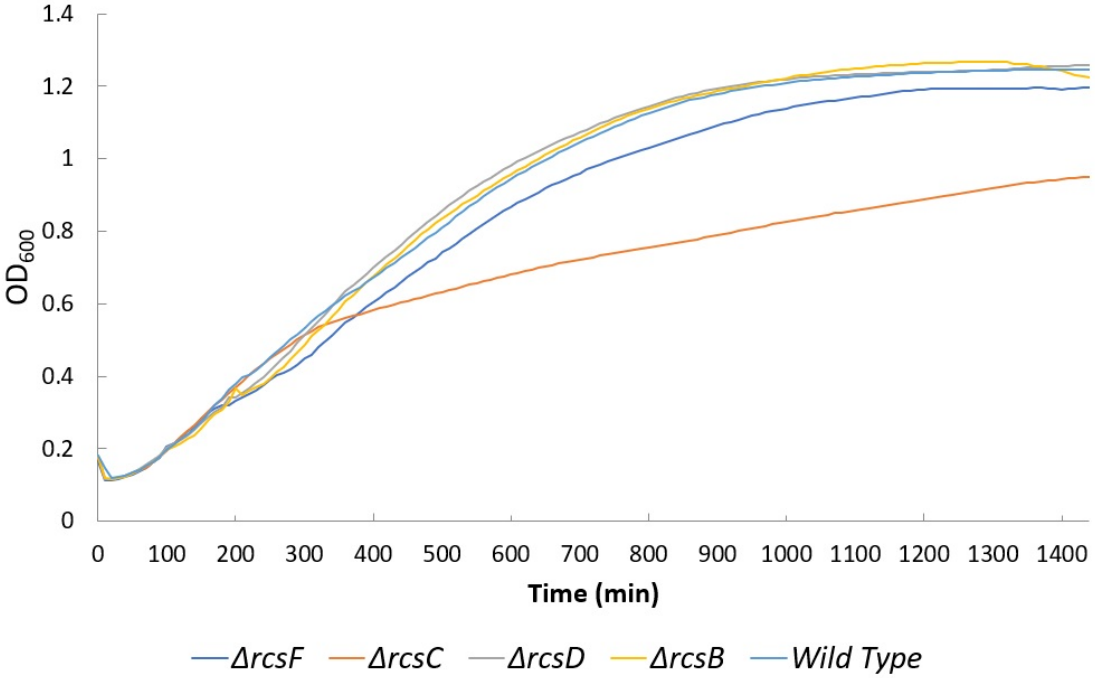

FIG. 4 Relative growth rates of Δ*rcs* mutants and WT. A growth curve of each Δ*rcs* mutant and WT was generated by measuring the optical density at 600 nm at 10-minute increments for 24 hours. This figure shows the growth rate of each mutant in an antibiotic absent condition.

DISCUSSION

The Rcs pathway in Enterobacteriaceae is considered to be a non-orthodox phosphorelay system due to the complexity of steps in signal transduction as seen in multiple input points and the multiple downstream pathways it feeds into (12). The response regulator RcsB and sensor kinase RcsC represent the two main components of the system (13). Jalalkamali *et al* demonstrated a previously proposed model suggesting signals from RcsC to RcsB are mediated by RcsD (Figure 1). IgaA, an inner membrane protein, under normal conditions inhibits RcsC autophosphorylation and therefore inhibits Rcs pathway activation. When RcsF, a resident of outer membrane porins, senses peptidoglycan damage it binds to IgaA which removes its inhibition to RcsC. This ultimately leads to downstream activation of RcsB (6). As a central component of the Rcs pathway, we focused on characterizing the Δ*rcs*C deletion *E. coli* mutant generated by Baba *et al* as part of the Keio Collection.

Using PCR and Sanger sequencing data from the Δ*rcsC* mutant, we verified the site of insertion of *kanR*. The Δ*rcsC* mutant is classified as a gene deletion in the Yale Coli Genetic Stock Center database, with an insertion of the *kanR* cassette in place of the deletion. Prior to this investigation, we assumed that such a deletion would encompass the entire gene, leading to a whole-gene knockout. As a result, we expected that PCR amplification using primers flanking the *rcsC* gene would generate a product of similar size to *kanR* (795 bp). Following agarose gel electrophoresis of the PCR products, however, a band size of roughly 4000 bp was observed (Figure 2). Further investigation was done using the primer set kanR-R/rcsC-R to amplify the region between *kanR* and the downstream region of the *rcsC* gene. This resulted in a slightly smaller band size of 3500 bp. Sequence analysis indicated that the cassette was inserted within the 5' region of the *rcsC* gene, and that only a portion of the *rcsC* gene was deleted. As the PCR-amplified *rcsC* product in WT was observed to be near 3000 bp in length, addition of the *kanR* cassette within the *rcsC* gene would result in a PCR product with band sizes similar to what was observed. We generated an insert map illustrating the precise location of insertion within the *rcsC* gene,

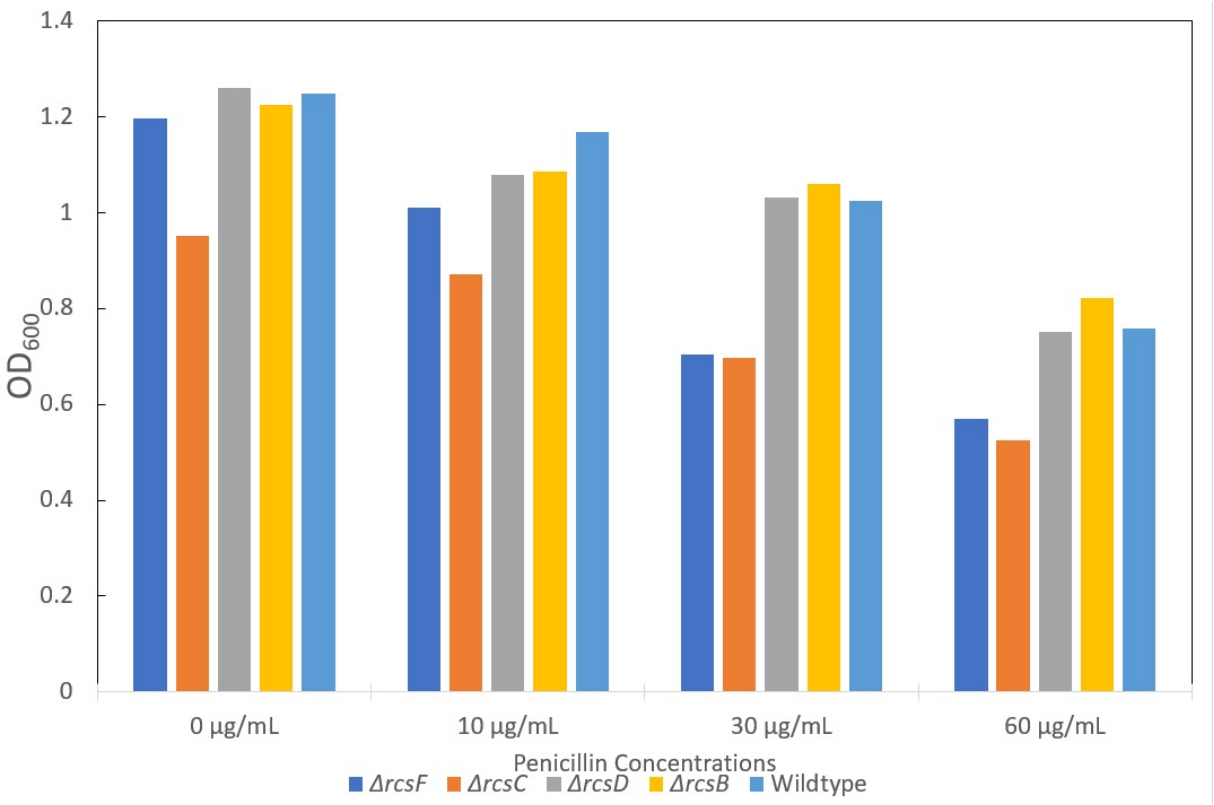

FIG. 5 Relative growth rates of different Δ*rcs* mutant strains at different concentrations of penicillin. Optical density at 600nm was measured at t=1400 minutes post growth analysis initiation. Each group represents a different penicillin concentration and each coloured bar represents a different Δ*rcs* mutant or WT.

and the remaining portion of the gene in the Δ*rcsC* mutant (Figure 3). The *kanR* insertion replaced the transcription initiation sequence for *rcsC*, and since the *kanR* contains its own transcription termination sequence there is no transcription of the remaining downstream portions of *rcsC*. Therefore, no functional RcsC protein is produced. Due to time constraints, the other Δ*rcs* mutants used in this study did not have their *kanR* insertion sites sequenced, and therefore we can only consider them as putative knockout mutants.

As stated previously, RcsC and RcsB compose the sensor kinase and response regulator components of the Rcs pathway, respectively. Other components investigated in our growth analyses were the outer membrane protein RcsF and the inner membrane protein RcsD. We compared knock out strains of each of these genes in a growth assay. In the absence of antibiotics, the Δ*rcsC* mutant showed a 2-fold lower growth yield over 24 hours compared to the WT strain, while the other mutants, including Δ*rcsB*, had comparable growth yields to WT. This supports that although a large portion of the *rcsC* gene remains in the Δ*rcsC* mutant genome, the deletion of the *rcsC* transcription initiation sequence and insertion of *kanR* was sufficient to knockout RcsC functionality. This also suggests that in conditions of no antibiotic stress loss of RcsC is deleterious to growth while loss of RcsB, RcsD and RcsF have little to no effect on growth. This ultimately suggests a broader role for RcsC in normal cell functioning compared to other Rcs pathway components, including RcsB. Therefore, we propose that RcsC does not act exclusively within the Rcs pathway but interacts with separate pathways that are important for cell growth under normal conditions.

Without penicillin treatment, the Δ*rcsF* mutant had growth characteristics comparable to WT (Figure 5). However, with increasing penicillin concentrations the growth yield of the Δ*rcsF* mutant decreased to be comparable to the Δ*rcsC* mutant, while the Δ*rcsB* and Δ*rcsD* mutants showed growth patterns similar to WT. This could be explained by the role of RcsF in recognition of peptidoglycan damage and loss of RcsF leading to an inability to appropriately respond to cell wall stress (6). However, if a defect in Rcs pathway activation were responsible for the observed phenotype of the Δ*rcsF* mutants we would expect to have seen a similar growth pattern in our other knockout mutants. Therefore, we suggest that presence of RcsF, regardless of the presence or absence of other Rcs pathway components, confers some intrinsic protection to β-lactam antibiotics. We suggest that inhibiting *rcsF* expression or antagonising RcsF could increase susceptibility of *E. coli* to β-lactam antibiotics, which may be especially useful in a medical setting and warrants further investigation.

Conclusions The *E. coli* K12 Δ*rcsC* mutant, JW5917-1, obtained from the Keio Collection has been studied for its growth characteristics in the presence and absence of penicillin. Insertion of the kanamycin-resistance cassette within this mutant has been mapped to a portion of the *rcsC* gene, generating a partial gene deletion but full loss of *rcsC* expression. The growth of the Δ*rcsC* mutant has been compared to the BW25113 WT and other Rcs pathway knockout mutants. The Δ*rcsC* mutant shows a distinct constraint on cellular growth. This may indicate the relative importance of RcsC in overall cellular function. The Δ*rcsF* mutant also shows reduced growth with increasing concentrations of penicillin, suggesting that RcsF may play an important role in protection from β-lactam antibiotics.

.

Future Directions Now that the Keio Collection *E. coli* K12 Δ*rcsC* mutant, JW5917-1, has had its growth characterized and *rcsC* locus sequenced it can be used to understand the mechanisms of the Rcs signalling pathway. Preliminary work into how the Rcs pathway influences the production of *rprA* in the presence of different antibiotics was conducted (results not shown). This was attempted using qPCR to measure the amount of *rprA* mRNA present in different antibiotic settings. Due to difficulties in validating the qPCR protocol there is no reproducible data available to answer this question. This is in part due to time constraints, as well as the small size of *rprA* mRNA. Reverse transcription is difficult with small RNA transcripts as the probability of transcribing the whole transcript is unlikely when using random primers. The primers we designed for qPCR were also at the end of the *rprA* mRNA sequence and thus we would need the full *rprA* transcript to be converted to cDNA to get a positive result in qPCR. Laubacher and Ades (2008) used a *lacZ* gene insertion downstream of the rprA promoter to quantify the expression of *rprA* mRNA

through measuring β-galactosidase activity in different antibiotic conditions. They may have used this method due to the small size of *rprA* mRNA and difficulties creating a qPCR product from cDNA and could explain our inconclusive results from the preliminary qPCR. Future researchers could combine these two experiments to identify how *rcsC* knockout affects *rprA* expression in different conditions.

The growth curve of different Δ*rcs* mutants incubated in penicillin suggests that the presence of Δ*rcsF,* regardless of downstream Rcs pathway products confers some resistance to penicillin. Future work could be conducted to repeat this experiment to improve the robustness of this argument and potentially understand how this pathway works. Addition of the *rcsF* gene into a gram-negative bacterial species that does not possess the Rcs signalling pathway and observing rescue from penicillin inhibition would support this argument.

ACKNOWLEDGEMENTS

We would like to thank the UBC Department of Microbiology and Immunology for providing the funding to allow us to execute this project. We would also like to thank Dr. Oliver and Mihai Cirstea for their guidance throughout this project. Finally, we would like to thank our fellow lab mates Hoang *et al* and Kovacevic *et al* for providing us with lab equipment and materials so we could execute our experiments.

CONTRIBUTIONS

The brainstorming, planning, and execution of the experiments, as well as the writing and editing of this paper were the result of the collective effort of all the authors. Some key contributions of each author include: KK: Primer design and growth curve data analysis; EM: Reagent generation and important lead in late PCR data; JM: Initial project proposal and important lead in PCR; MT: Key writing lead and growth curve preparation.

REFERENCES

1. **Laubacher ME, Ades SE**. 2008. The Rcs phosphorelay is a cell envelope stress response activated by peptidoglycan stress and contributes to intrinsic antibiotic resistance. J Bacteriol 190:2065-74.
2. **Richter L, Johnston A, Lam A.** 2016. The Rcs phosphorelay system and RcsB regulated *rprA* contributes to the intrinsic antibiotic resistance of *Escherichia coli* exposed to antibiotics targeting the cell wall. JEMI+ 1:42-48.
3. **Jalalkamali Y, Malekafzali N, Shabbir R, Sihota T**. 2018. The RcsB-dependent upregulation of *rprA* contributes to the intrinsic antibiotic resistance of *Escherichia coli* exposed to antibiotics targeting cell wall synthesis but not protein synthesis. JEMI+ 4:1-10.
4. **Storvik KA, Foster PL.** 2010. RpoS, the stress response sigma factor, plays a dual role in the regulation of *Escherichia coli*'s error-prone DNA polymerase IV. J Bacteriol 192:3639-44.
5. **Huang YM, Kan B, Lu Y, Szeto S**. 2009. The effect of osmotic shock on RpoS expression and antibiotic resistance in *Escherichia coli*. JEMI 13:13-17.
6. **Wall E, Majdalani N, Gottesman S**. 2018. The Complex Rcs Regulatory Cascade. Annu Rev Microbiol 72:111-139.
7. **Kelley WL, Georgopoulos C**. 1997. Positive control of the two-component RcsC/B signal transduction network by DjlA: a member of the DnaJ family of molecular chaperones in *Escherichia coli*. Mol Microbiol 25:913-31.
8. **Potrykus J, Wegrzyn G.** 2004. The ypdI gene codes for a putative lipoprotein involved in the synthesis of colanic acid in *Escherichia coli*. FEMS Microbiol Lett 235:265-71.
9. **Markova JA, Anganova EV, Turskaya AL, Bybin VA, Savilov ED.** 2018. Regulation of *Escherichia coli* biofilm formation (review). Appl Biochem Microbiol 54:1-11.
10. **Farris C, Sanowar S, Bader MW, Pfuetzner R, Miller SI.** 2010. Antimicrobial peptides activate the Rcs regulon through the outer membrane lipoprotein RcsF. J Bacteriol 192:4894-903.
11. **Baba T, Ara T, Hasegawa M, Takai Y, Okumura Y, Baba M, Datsenko KA, Tomita M, Wanner BL, Mori H.** 2006. Construction of *Escherichia coli* K-12 in-frame, single-gene knockout mutants: the Keio collection. Mol Syst Biol 2:2006 0008.
12. **Guo XP, Sun YC.** 2017. New Insights into the Non-orthodox Two Component Rcs Phosphorelay System. Front Microbiol 8:2014.
13. **Majdalani N, Gottesman S.** 2005. The Rcs phosphorelay: a complex signal transduction system. Annu Rev Microbiol 59:379-405.